Continuous Synthesis of Fuel Additives Alkyl Levulinates via Alcoholysis of Furfuryl Alcohol over Silica Supported Metal Oxides

Raji Reddy Chada[1] · Kumara Swamy Koppadi[1] · Siva Sankar Enumula[1] · Murali Kondeboina[1] · Seetha Rama Rao Kamaraju[1] · David Raju Burri[1]

Abstract

Aiming at synthesizing alkyl levulinates via alcoholysis of furfuryl alcohol in continuous mode for the first time an attempt is made using cheapest and eco-friendly solid acid catalysts. Different silica supported solid acid catalysts containing the oxides of aluminium, tungsten, zirconium and titanium have been prepared. The nature, number and strength of surface acidic sites were evaluated by DRIFT spectroscopy with pyridine adsorption and NH_3-TPD and also structural and textural features of the catalysts have been investigated by XRD and BET surface area techniques. Al_2O_3/SiO_2 catalyst exhibited better activity with 100% conversion of furfuryl alcohol and 92.8% selectivity of methyl levulinate, which may be due to more number of surface acidic sites with large number of weak Lewis acidic sites. The catalytic activity of these solid acid catalysts is as follows: $Al_2O_3/SiO_2 > ZrO_2/SiO_2 > WO_3/SiO_2 > TiO_2/SiO_2$. This is well correlated with the number of surface acidic sites. The stable catalytic activity during the 10 h time-on-stream study confirmed the sturdiness of Al_2O_3/SiO_2 catalyst and also it is active for the selective formation of ethyl, *n*-propyl, *n*-butyl levulinates.

Graphical Abstract
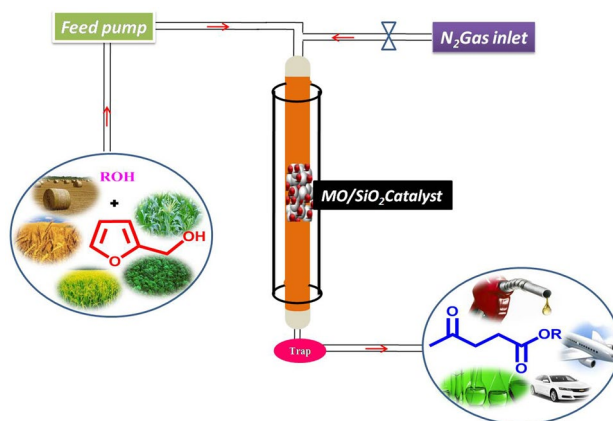
1 Introduction

Ever increasing environmental concerns and dependence on dwindling fossil resources for energy, persuading the research activities towards the alternative energy sources is essential [1]. Among the existing renewable energy sources, lignocellulosic biomass is a promising renewable

✉ David Raju Burri
david.iict@gov.in

[1] Department of Catalysis and Fine Chemicals, Indian Institute of Chemical Technology, Hyderabad 500007, India

feedstock for the green and sustainable production of bio based chemicals and 2nd generation bio fuels and is one of the approaches to reduce environmental pollution to some extent. Lignocellulosic biomass is the most abundant in agriculture residues and waste streams and is inexpensive, biodegradable and sustainable nature and in addition it avoids the production of first generation fuels from sugars, starch and vegetable oils. For the production of fuels via utilization of first generation feed stocks creates negative impacts like food versus fuel problems [2]. Lignocellulosic biomass is mainly composed of three biopolymers such as cellulose (40–50%), hemicellulose (25–30%) and lignin (15–20%). Cellulose and hemicellulose polymers easily convert into their respective monomeric sugars by lower energetic C–O (glycoside) bond cleavage. These sugars can be further converted into fuels, fuel additives and chemicals in multiple steps through various possible platform molecules [3–5]. Furfural is considered as an excellent platform molecule, which can be easily converted into furfuryl alcohol (FAL) over Cu/MgO and carbon–MgO catalysts in continuous process [6, 7]. The alcoholysis of FAL to alkyl levulinates (AL) has gained particular attention due to their potential applications in transportation fuel, perfumery and flavouring industries [2, 8]. AL are the main precursor for the synthesis of valuable chemicals, such as γ-valerolactone. AL can also be used as additives in gasoline and diesel transportation fuels, which create enviable properties like cleaner combustion, high lubricity, conductivity, decrease in emission of toxic gases and particulate matter and also flow properties even under cold conditions [9–11]. On the basis of physical properties AL can be used as blending agents for diesel. The blending of 20% ethyl levulinate (EL) to cotton seed oil improves the fuel properties [12]. The swelling of engines and percent hardness can be reduced with butyl levulinate (BL) and higher AL. EL (10 v/v%) and BL (20 v/v%) were blended with diesel fuel and tested for Cummins ISB engine and observed that engine-out smoke was reduced by 41.3 and 55% respectively [11]. AL have been proposed as green solvents due to lower vapour pressures compare to chlorinated solvents and based on this property, Ferrer et al. claimed that these can be used in metallic degreasing processes instead of industrially used harmful trichloroethylene [13]. Conventionally, AL have been synthesized by using inorganic liquid acids such as HCl, H_2SO_4, H_3PO_4 and HF. However, the complications like corrosiveness, recyclability and environmental issues hinder their industrial applications [14]. To overcome these drawbacks, scientific community has made several attempts to develop sustainable approaches for the production of AL in green process and many researchers have been explored the synthesis of AL from alcoholysis of FAL over various solid acid catalysts. The most of reported catalytic systems involve catalysts like ion exchange resins [15], mesostructured aluminosilicates [16], sulfated metal oxides [17], Al-TUD-1 [18], sulfonic acid functionalized materials of carbon [19], ionic liquids and organosulfonic acid functionalized SBA-15 [20, 21], organosilica hollow nanospheres [22], zirconia bi-functionalized organosilica modified heteropoly acid [23] and $ZnTPA/Nb_2O_5$ [24]. Even though those catalytic systems offer good catalytic activity, the difficulty in preparation and usage of expensive precursors are one of the drawbacks. Furthermore, most of these reactions are conducted in batch conditions, in which, longer reaction times, catalyst separation from reaction mixture, disposal of effluents and reuse of catalyst are the notable difficulties, which are unavoidable process limitations. In this context, the production of AL in continuous process at atmospheric pressure over facile, inexpensive, efficient, stable and eco-friendly solid acid catalytic systems is more advantageous.

It has reported that, the alcoholysis of FAL to produce alkyl levulinates is significantly influenced by the acid site density, strength and accessibility of active sites to reactants [8, 25]. Hence, in the present investigation, preparation of Al_2O_3/SiO_2, WO_3/SiO_2, ZrO_2/SiO_2, TiO_2/SiO_2 solid acid catalysts, determination of structural and textural characteristics, estimation of type, distribution, nature and strength of acidic sites and their correlation with the alcoholysis of furfuryl alcohol in the formation of alkyl levulinates in the fixed bed reactor has been delineated.

2 Experimental

2.1 Preparation of Various Solid Acid Catalysts

Various solid acid catalysts such as Al_2O_3/SiO_2, ZrO_2/SiO_2, WO_3/SiO_2 and TiO_2/SiO_2 were prepared by wet impregnation method using SiO_2 (Aldrich Chemicals, USA) as support and $Al(NO_3)_3 \cdot 9H_2O$ (S.D. Fine-Chem. India), $H_{26}N_6O_{40}W_{12} \cdot xH_2O$ (Aldrich Chemicals, USA), $ZrO(NO_3)_2 \cdot xH_2O$ (S.D. Fine-Chem. India) and $TiCl_4$ (Chemlabs, India) are as precursors for Al_2O_3, WO_3, ZrO_2 and TiO_2 respectively. In a typical method, requisite amount (10% by weight) of the metal precursor dissolved in water was mixed with SiO_2 by continuous stirring and the mixture was dried under constant manual stirring up to complete dryness. The solid was dried in an air oven at 100 °C for 12 h, and then calcined at 500 °C for 4 h in static air. The calcined Al_2O_3/SiO_2, ZrO_2/SiO_2, WO_3/SiO_2 and TiO_2/SiO_2 are designated as AS, ZS, WS and TS respectively, which are collectively known as MO/SiO_2.

2.2 Characterization

All of these catalysts were characterized by different techniques. The X-ray patterns were recorded on an Ultima-IV

(M/s. Rigaku Corporation, Japan) XRD unit operated at 40 kV and 40 mA equipped with Ni-filtered Cu Kα radiation (λ = 1.54056 Å) in the 2θ range of 10°–80° at a scanning rate of 0.02° per step at room temperature. Elemental analysis was made on ICP-OES (M/s. Thermo Scientific iCAP6500 DU) by dissolving in aqua regia along with few drops of hydrofluoric acid. BET surface area measurements were made on a Quadrusorb-SI V 5.06, adsorption unit (M/s. Quantachrome Instruments Corporation, USA) by N_2 adsorption at − 196 °C. The samples were out-gassed at 200 °C for 4 h before the measurement. The acidity of the catalysts was measured by temperature programmed desorption of NH_3 using an AUTOSORB-iQ automated gas sorption analyzer (M/s. Quantachrome Instruments, USA). Prior to desorption, the catalyst has been saturated with NH_3 at 60 °C for 0.5 h, followed by flushing with helium for 0.5 h to flush off the physisorbed NH_3 at the same temperature. Then, the temperature was raised to 800 °C at 10 °C min^{-1} and the desorbed NH_3 was monitored with the inbuilt TCD in a flow of helium (60 mL min^{-1}). The pyridine adsorption spectra were recorded in the diffuse reflectance infra red Fourier transform (DRIFT) mode. Prior to adsorption of pyridine the catalysts were degassed under vacuum at 200 °C for 3 h and followed by the removal of excess pyridine by heating the sample at 120 °C for 1 h. Then FT-IR spectra of the pyridine-adsorbed samples were recorded at room temperature.

2.3 Activity Measurement

The catalytic activity experiments were conducted in a fixed bed quartz reactor (14 mm id and 280 mm length) at atmospheric pressure. In each catalytic experiment, 250 mg of catalyst is diluted with equal amount of quartz particles and placed at the centre of the reactor. Prior to the reaction, the catalyst was flushed in a N_2 flow of 1800 mL h^{-1} at 180 °C for 1 h. The liquid feed with required molar ratio of FAL to alcohol was continuously fed at a liquid hour space velocity (LHSV) of 1 h^{-1} using a feed pump (M/s. B. Braun Co., Germany). Unless otherwise specified the reaction conditions are same. The liquid product mixture was collected in an ice cold trap and analyzed at regular intervals. This product mixture was analyzed by a flame ionization detector (FID) equipped gas chromatograph, GC-17A (M/s. Shimadzu Instruments, Japan) with EB-5 capillary column (30 m × 0.53 mm × 5.0 μm) and the product components were confirmed by using GC–MS, QP-2010 (M/s. Shimadzu Instruments, Japan) with EB-5 MS capillary column (30 m × 0.25 mm × 0.25 μm).

3 Results and Discussions

The powder XRD patterns of MO/SiO_2 catalysts were depicted in Fig. 1. A broad characteristic peak of amorphous silica was observed in the vicinity of 2θ = 15°–30° in all catalysts. The absence of characteristic diffractions of crystalline Al_2O_3 and ZrO_2 in AS and ZS catalysts, imply that these two metal oxide are in amorphous form or in highly dispersed form (i.e., below the instrument sensitivity limit < 5 nm). In WS catalyst diffractions at 2θ = 23.13°, 23.58°, 24.35°, 26.39°, 28.65°, 33.35°, 41.60°, 49.92° and 55.73° are due to WO_3 with monoclinic phase (JCPDS No 72-0677) [26]. In TS sample 2θ = 25.30°, 48.10° and 55.13° diffraction lines represent the presence of TiO_2 in tetragonal phase (JCPDS No 83-2243). The presence of Al_2O_3 and ZrO_2 are evidenced from ICP-OES analysis and the values are presented in Table 1, which are close to the theoretical values. The BET surface area of silica supported metal oxide catalysts displayed in Table 1. The surface area of these catalysts found to be in the range of 176–263 m^2 g^{-1}. AS and ZS catalysts are having more surface area than those of WS and TS catalysts. Higher surface area of AS and ZS catalysts ascribed from porous nature of highly dispersed respective metal oxide over the silica support. NH_3-TPD profiles of MO/SiO_2 catalysts were displayed in Fig. 2 and the respective acidity values are given in Table 1. The acidic sites distribution according to strength was classified depending upon desorption temperature of chemisorbed NH_3 as weak (< 250 °C), moderate (250–400 °C) and strong (> 400 °C) acidic sites [27, 28]. Pure silica did not show any appreciable amount of NH_3 desorption but MO/SiO_2 samples show significant amount of NH_3 desorption. It indicates that the
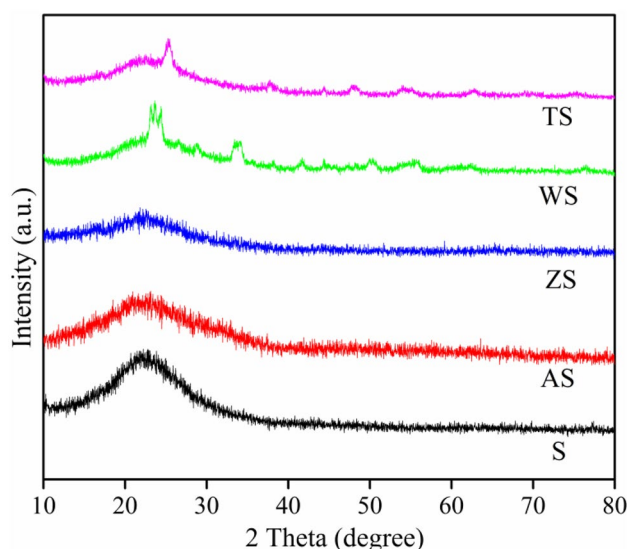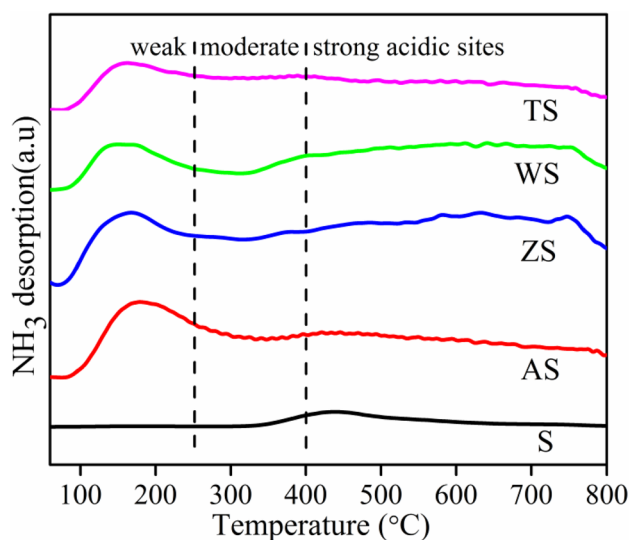

**Fig. 1** XRD patterns of various MO/SiO_2 catalysts

Table 1 Textural properties of various metal oxide supported catalysts

Sample	S_{BET} $(m^2 g^{-1})^a$	Theoretical metal oxide loading (wt%)	Metal oxide loading by ICP-OES	Acidity (NH_3 m mol $g^{-1})^b$
S	300	–	–	0.01
AS	263	10.0	9.6	0.76
WS	230	10.0	9.6	0.50
ZS	251	10.0	9.5	0.66
TS	176	10.0	9.4	0.36

[a]BET surface area

[b]Total acidity obtained from TPD of NH_3

Fig. 2 NH_3-TPD patterns of various MO/SiO$_2$ catalysts

MO deposition on SiO_2 support generated the acidic sites. Weak acidic sites are observed in all MO/SiO$_2$ catalysts. AS catalyst showed a prominent desorption peak in the region of 80–290 °C signifying the presence of more number of weak acidic sites [29]. Two desorption peaks are observed in WS catalyst, which related to weak and strong acidic sites. ZS catalyst possessed more number of weak acidic sites along with some strong acidic sites. TS catalyst showed desorption peak in the temperature region of 80–250 °C, indicates the presence weak acidic sites. However, AS catalyst possess more number of acidic sites among the MO/SiO$_2$ catalysts.

Pyridine adsorbed FT-IR spectroscopy was used to evaluate nature of surface acidic sites present in catalysts and the respective recorded spectra are presented in Fig. 3a. These spectra show the formation of bands due to co-ordinated pyridine at 1445 and 1580 cm^{-1}. The other band in the spectrum at 1489 cm^{-1} is ascribed from combination of protonated and co-ordinated pyridine. In order to know the stability of the
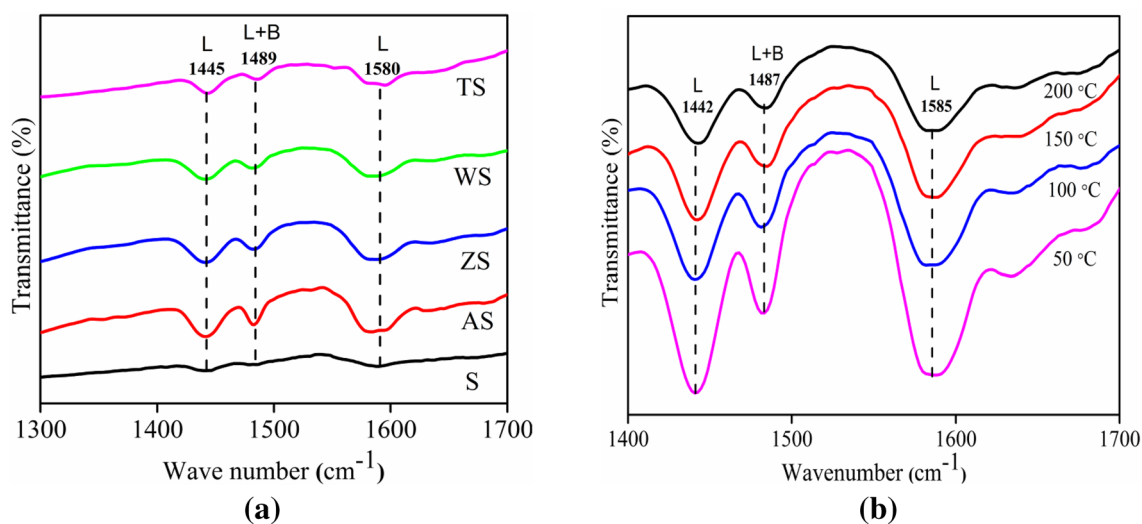
Fig. 3 **a** Py-FTIR spectra of various MO/SiO$_2$ catalysts. **b** Pyridine desorption spectra of AS catalyst at different temperatures

acidic sites, pyridine desorption spectra of the active catalyst (AS) at different temperature was recorded and presented in Fig. 3b. The intensities of corresponding bands representing the Lewis acidic sites are decreasing with rise in temperature from 50 to 200 °C due to loss of some amount of pyridine. NH_3-TPD analysis results are good agreement with pyridine adsorbed DRIFT FT-IR spectroscopy. In the case of ZS, WS and TS catalysts low intense bands are observed compared to AS which is due to lower number of acidic sites.

3.1 Activity Studies

3.1.1 Performance of Silica Supported Metal Oxide Catalysts

The vapour phase alcoholysis of FAL with methanol was carried out over different SiO_2 supported metal oxide (Al_2O_3, ZrO_2, WO_3 and TiO_2) catalysts at atmospheric pressure at 180 °C temperature (The boiling point of furfuryl alcohol is 170 °C, hence, the minimum operating temperature of this reaction is set at 180 °C) and results are presented in Fig. 4. The alcoholysis of FAL to alkyl levulinates is shown in Scheme 1. The pure silica exhibited very poor catalytic activity, i.e., 8% conversion of FAL and 2%
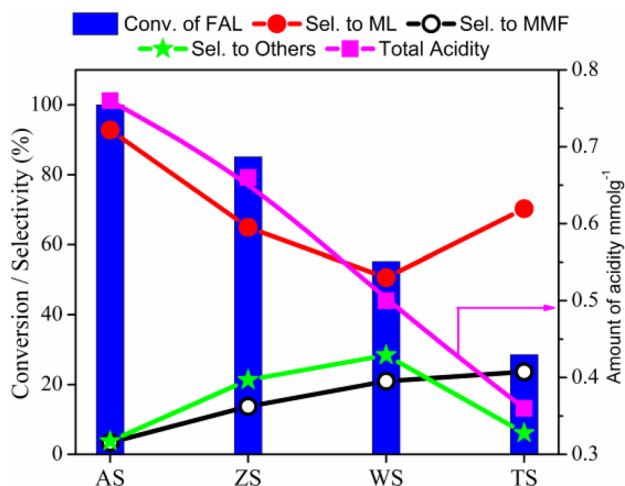
selectivity of ML. The AS catalyst showed better activity with close to 100% conversion of FAL and the selectivities of ML and 2-methoxy methyl furan (MMF) are 92.8 and 3.4% respectively. MMF is an intermediate in the formation of ML (Scheme 1). With other catalysts like ZS, WS and TS catalysts, the conversions are 85.1, 55.2 and 28.6% with 65.0, 50.6, and 70.3% selectivities of ML respectively. In the catalytic activity point of view, MO/SiO_2 catalysts are far more superior compared to silica support, which might have imparted from the creation of Lewis acidic sites (Fig. 3a). The notable variation in the catalytic activity among the catalysts seems to depend on the strength and distribution of accessible acidic sites. The conversion of FAL and selectivity to ML declined and selectivity of MMF increased with decreasing the total acidity of the catalysts. The increase in selectivity to MMF presumably due to insufficient accessible acidic sites impede the rate of FAL alcoholysis, thereby accumulation of intermediate MMF on active sites takes place. Comparatively, WS and TS catalysts exhibited poor catalytic performance due to low dispersion of WO_3 and TiO_2 on silica support (confirmed from Fig. 1) which results in lower number of acidic sites evidenced from NH_3-TPD results (Table 1). Indeed, the active sites for this reaction are acidic sites and also their distribution towards strength. Weak acidic sites are responsible for the formation of ML from FAL whereas strong acidic sites are responsible for by-products. High by-product selectivity at the cost of ML for WS sample is due to the presence of strong acidic sites which are absent in TS sample (Fig. 2). From these results AS catalyst found to be best catalyst among these MO/SiO_2 catalysts in terms of conversion and ML selectivity. The superior catalytic activity of AS catalyst mainly contributed from presence of more number of weak Lewis acidic sites. Therefore further activity studies were carried out over AS catalyst and the results are presented in the subsequent sections.

3.1.2 Influence of Molar Ratio

In order to know the influence of molar ratio of FAL to methanol on the activity of AS catalyst with respect to conversion of FAL and selectivity of ML and the results are shown in Fig. 5. The FAL to methanol molar ratio was varied from 1:5 to 1: 25. The selectivity to ML increased
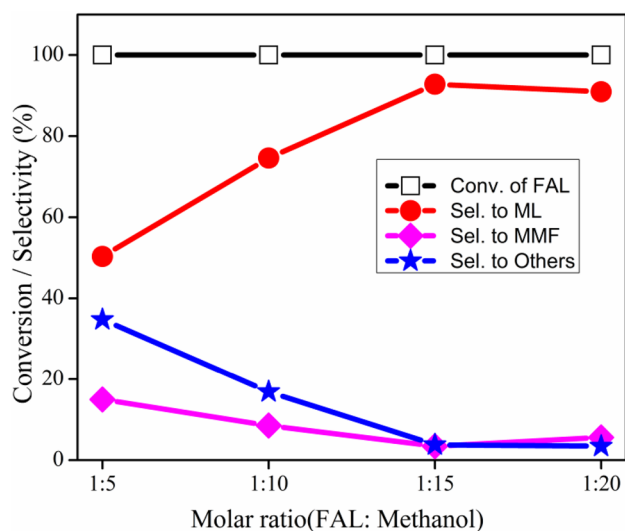

Fig. 4 Influence of different MO/SiO_2 catalysts on FAL alcoholysis with methanol. Reaction conditions: FAL:methanol = 1:15 mol ratio; reaction temperature: 180 °C; N_2 flow: 30 mL min^{-1}; LHSV: 1 h^{-1}

Scheme 1 Conversion of furfuryl alcohol with various alcohols to alkyl levulinates via 2-alkoxy methylfuran

Furfuryl alcohol

2-Alkoxy methylfuran

Alkyl levulinates

R= CH_3, C_2H_5, C_3H_7, C_4H_9

Fig. 5 Influence of molar ratio of FAL to methanol on alcoholyis over AS catalyst. Reaction conditions: FAL:methanol = 1:5–1:20 mol ratio; reaction temperature: 180 °C; N_2 flow: 30 mL min^{-1}; LHSV: 1 h^{-1}
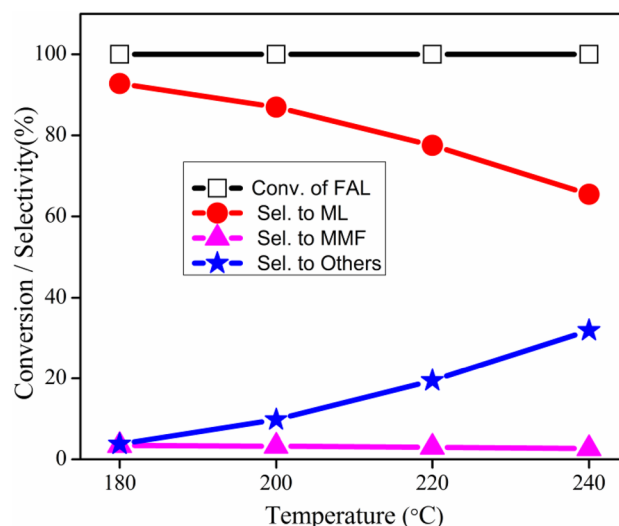

Fig. 6 Effect of temperature on alcoholyis of FAL with methnol over AS catalyst. Reaction conditions: FAL:methanol = 1:15 mol ratio; reaction temperature: 180–240 °C; N_2 flow: 30 mL min^{-1}; LHSV: 1 h^{-1}

with increase in molar ratio of FAL to methanol from 1:5 to 1:15 and attained a maximum selectivity of ML (92.8%) at a molar ratio of 1:15. Further increase in the molar ratio to 1:20, no considerable change in ML selectivity was observed. At lower FAL to methanol molar ratios the FAL readily underwent polymerization and produced the oligomers [30]. To minimize the formation of oligomeric products, higher amount of methanol is required. These results suggested that the maximum ML selectivity was achieved at 1:15 FAL to methanol molar ratio.

3.1.3 Effect of Temperature

To investigate the influence of temperature on the alcoholysis FAL to ML, the experiments were conducted at different temperatures from 180 to 240 °C over AS catalyst and the results are depicted in Fig. 6. The conversion of FAL is found to be 100% at all the temperatures, but selectivity to ML varied with temperature. With increasing reaction temperature from 180 to 240 °C, ML selectivity is decreased due to formation of by-products such as FAL oligomers and angelica lactones. According to reported literature angelica lactones formation is from either FAL or MMF [31]. Based on these activity results, the optimum reaction temperature for the alcoholysis of FAL is 180 °C.

3.1.4 Effect of Liquid Hour Space Velocity (LHSV)

The effect of LHSV on FAL alcoholysis over AS catalyst was examined in the range of 1–6 h^{-1} and the results were depicted in Fig. 7. As the LHSV changed from 1 to

6 h^{-1} there is no change in the FAL conversion, but ML selectivity significantly decreased due to enhancement of MMF selectivity. Indeed, the MMF is intermediate for the formation of ML from FAL through rehydration. However, maximum ML selectivity was achieved at 1 h^{-1} LHSV.
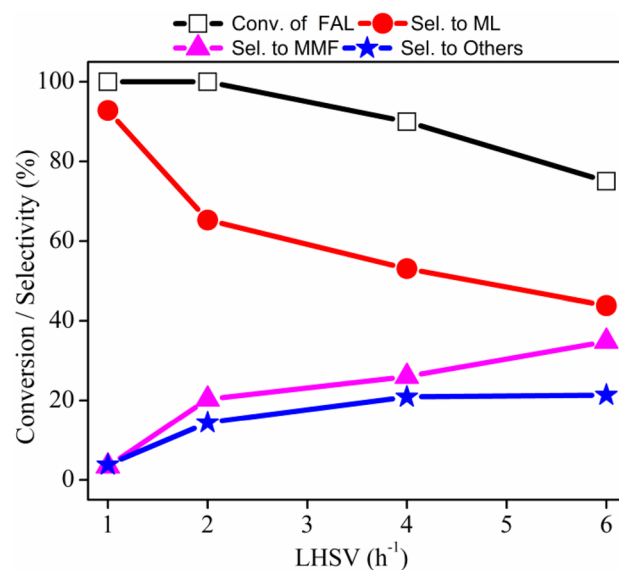

Fig. 7 Influence of liquid hour space velocity on FAL alcoholysis with methanol over AS catalyst. Reaction conditions: FAL:methanol = 1:15 mol ratio; reaction temperature: 180 °C; N_2 flow: 30 mL min^{-1} LHSV: 1–6 h^{-1}
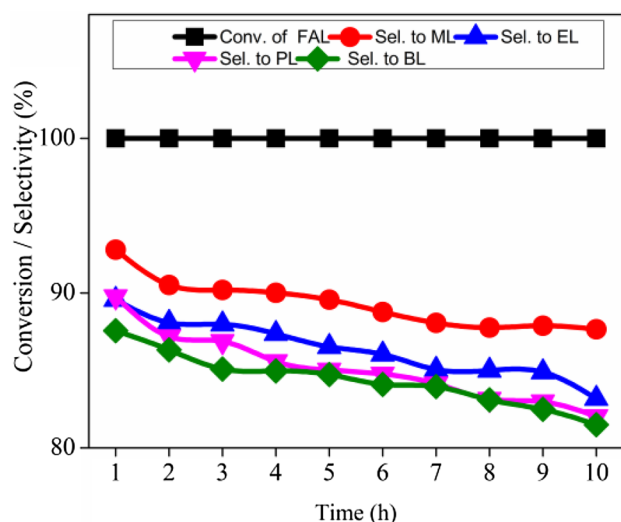
Fig. 8 Influence of time on stream on FAL alcoholysis with various alcohols over AS catalyst. Reaction conditions: FAL:alcohol = 1:15 mol ratio; reaction temperature: 180 °C, N_2 flow: 30 mL min^{-1}; LHSV: 1 h^{-1}
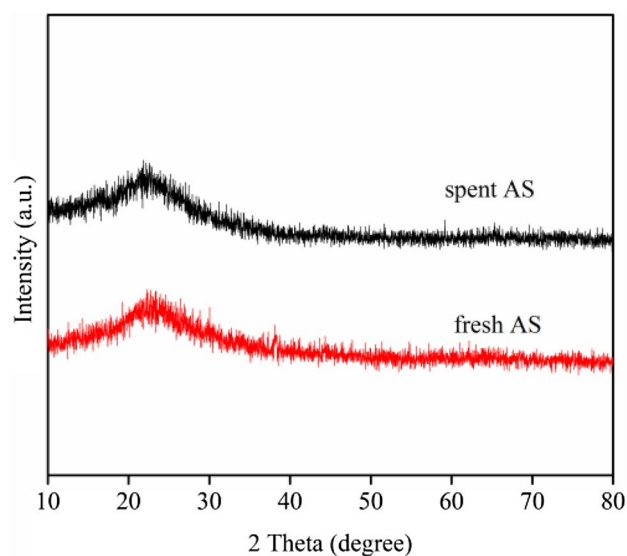

Fig. 9 XRD patterns of fresh and spent AS catalysts

3.1.5 Time on Stream Activity Study (TOS)

AS catalyst longevity test was performed under the optimized reaction conditions for the alcoholysis of FAL to ML and the results were shown in Fig. 8, which showed the steady catalytic activity during 10 h time-on-stream. Up to 10 h, the conversion of FAL is constant (100%), while selectivity to ML declined slightly. To know the reasons for slight decrease in ML selectivity, spent catalysts was analyzed by XRD, NH_3-TPD, CHNS and TGA techniques. The XRD patterns of fresh and spent AS catalysts (Fig. 9)
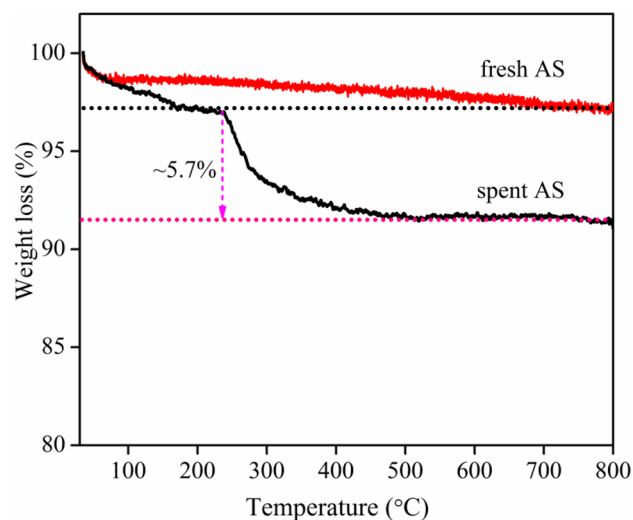

Fig. 10 TGA analysis of fresh and spent AS catalyst

Table 2 Coke formation and acidity of catalysts

Catalyst	Carbon, wt% (CHNS)	Carbon, wt% (TGA)	Acidity (NH_3 m mol g^{-1})
Fresh AS	0	0	0.76
Spent AS	4.4	5.7	0.63

showed no significant changes. A comparison made between NH_3-TPD profiles of fresh and spent AS catalysts, illustrating the lowering of total acidity from 0.76 to 0.63 mmol g^{-1}. CHNS and TGA analysis (Fig. 10) of the fresh and spent AS catalyst presented in Table 2, confirming the deposition of coke on the spent catalyst. The amount of coke obtained from either CHNS or TGA is more or less constant. Because of coke deposition, lowering in total acidity was observed, as resultant, the selectivity of ML decreased. However, the catalyst is robust at least up to 10 h of TOS.

3.1.6 Effect of Various Alcohols

To examine the performance of AS catalyst on FAL alcoholysis to ML with different alcohols under the optimized reaction conditions was investigated and the results are shown in Fig. 8. The conversion of FAL is 100% with ethanol, propanol and butanol but the selectivity to ethyl levulinates, propyl levulinates and butyl levulinates was decreased slightly during the course of TOS (10 h). The AL selectivity is found to decrease slightly with increase in alcohol chain length from ethanol to butanol. It is also found that formation of γ-valerolactone (3–5%) is observed when ethanol, 1-propanol and 1-butanol were used as alcohol source in FAL alcoholysis.

4 Conclusions

Alkyl levulinates are synthesized in continuous mode successfully from alcoholysis of furfuryl alcohol over facile, cheap and eco-friendly solid acid catalysts such as Al_2O_3/SiO_2, ZrO_2/SiO_2, WO_3/SiO_2 and TiO_2/SiO_2, of which Al_2O_3/SiO_2 showed better catalytic activity through its weak Lewis acidic sites nature and number.

References

1. Ahmad E, Alam MI, Pant KK, Haider MA (2016) Green Chem 18:4804
2. Sankar ES, Babu GVR, Reddy CR, Raju BD, Rama Rao KS (2017) J Mol Catal A 426:30
3. Climent MJ, Corma A, Iborra S (2014) Green Chem 16:516
4. Kobayashi H, Fukuoka A (2013) Green Chem 15:1740
5. Climent MJ, Corma A, Iborra S (2011) Green Chem 13:520
6. Nagaraja BM, Padmasri AH, David Raju D, Rama Rao KS (2017) J Mol Catal Chem 265:90
7. Swamy KK, Reddy CR, Sankar ES, Kumar MR, Rama Rao KS, Raju BD (2017) Catal Lett 147:1278
8. Demolis A, Essayem N, Rataboul F (2014) ACS Sustain Chem Eng 2:1338
9. Janssen A, Pischinger S, Muether M (2010) SAE Int J Fuels Lubr 3:70
10. Clark RH, Groves AP, Morley C, Smith J (2004) Fuel compositions. Patent WO2004035713
11. Christensen E, Williams A, Paul S, Burton S, McCormick RL (2011) Energy Fuels 25:5422
12. Joshi H, Moser BR, Toler J, Smith WF, Walker T (2011) Biomass Bioenergy 35(7):3262
13. Ferrer NB, Prats LG, Company CE, Boliart JC (2013) European. Patent EP2540871A1
14. Leng Y, Wang J, Zhu DR, Ren XQ, Ge HQ, Shen L (2009) Angew Chem Int Ed 121:174
15. Lange JP, van de Graaf WD, Haan RJ (2009) ChemSusChem 2:437
16. Neves P, Antunes MM, Russo PA, Abrantes JP, Lima S, Fernandes A, Pillinger M, Rocha SM, Ribeiro MF, Valente AA (2013) Green Chem 15:3367
17. Zhao G, Hu L, Sun Y, Zeng X, Lin L (2014) BioResources 9:2634
18. Neves P, Antunes MM, Russo PA, Valente AA (2013) Green Chem 15:3367–3376
19. Liu RL, Chen JZ, Huang X, Chen LM (2013) Green Chem 15:2895
20. Wang G, Zhang Z, Song L (2014) Green Chem 16:1436
21. Car PD, Ciriminna R, Shiju NR, Rothenberg G, Pagliaro M (2014) ChemSusChem 7:835
22. Lu B, An S, Song D, Su F, Yang X, Guo Y (2015) Green Chem 17:1767
23. Song D, An S, Sun Y, Guo Y (2016) J Catal 333:184
24. Rao BS, Kumari PK, Dhanalakshmi D, Lingaiah N (2017) J Mol Catal A 427:80
25. Neves P, Lima S, Pillinger M, Rocha SM, Rocha J, Valente AA (2013) Catal Today 76:218
26. Rajesh B, Subratanath K (2012) Inorg Chim Acta 384:233
27. Boreave A, Auroux A, Guimon C (1997) Microporous Mater 11:275
28. Reddy CR, Thirupathaiah K, Reddy BA, Devi GS, Rao KSR, Raju BD (2017) Mol Catal 438:224
29. Feng P, Xuchen L, Qingshan Z, Zhimin Z, Yan Y, Tizhuang W, Shiwei C (2015) J Mater Chem A 3:4058.
30. Mija A, Navard P, Peiti C, Babor D, Guigo N (2010) Eur Polym J 46:1380
31. Khusnutdinov R, Baiguzina A, Smirnov A, Mukminov R, Dzhemilev U (2007) Russ J Appl Chem 80:1687